ELSEVIER

Chemical Engineering Journal 86 (2002) 153–164

Chemical Engineering Journal

www.elsevier.com/locate/cej

Recent advances in pore-scale models for drying of porous media

M. Prat*

Institut de Mécanique des Fluides de Toulouse, UMR CNRS-INP/UPS No. 5502, Avenue du Professeur Camille Soula, 31400 Toulouse, France

Abstract

This paper presents a review of the recent advances in pore-scale modelling of drying in capillary porous media. The development of pore network models in drying has been first motivated by several fundamental features of drying that cannot be fully explained within the framework of continuum models. These features include the dry patch phenomenon and the constant drying rate period. A second source of motivation has been the advances made in pore-scale modelling of immiscible displacements in porous media and the increasing conviction that concepts developed in this area could be utilised to model drying. These concepts are recalled. We describe how they have been used for developing a pore network model of drying driven by mass transfer. A review of the main results is made, including pattern formation, drying rates and some recent results regarding drying of a porous medium containing a binary mixture and the influence of heat transfer. The use of network models for computing effective transport properties is discussed. Open problems are discussed.

Keywords: Capillary porous media; Pore networks; Simulation; Pure and binary liquids; Percolation theory

1. Introduction

The development of models for drying of porous media has been the subject of many studies, see for instance [1–3]. Motivations are numerous and varied. This is due to the fact that there exists a great variety of drying processes and that drying can be considered at different scales (typically from the pore-scale to the dryer scale). For a given drying process, one can reasonably put forward that a model relevant at a given scale should be consistent with the models describing drying at smaller scales. Hence, modelling at the dryer scale can be envisioned as an upscaling problem. This somewhat ideal vision implies that the modelling should be initiated at the first scale of interest, typically the pore-scale, and that models at larger and larger scales are successively developed up to the dryer scale. Naturally, design of dryers is far from being the sole motivation for developing models at the product scale, see [1,4]. In any case, a correct modelling of drying at the product scale is of interest. The nature of the product is also a great source of diversity, from inert materials to foodstuffs. One possible classification is to consider how water is fixed in the product. Above a concept of pore was implicitly assumed. Furthermore, we assume that water can be fixed only within the pores, i.e. water fixed in the solid matrix, if any, is not considered. Traditionally, two modes of fixation are considered: adsorption and capillarity [4–6]. Materials in which a large amount of water can be fixed by adsorption are termed hygroscopic materials while materials in which water is essentially fixed by capillarity form the capillary porous media. In this paper, we are primarily concerned with rigid capillary materials. This special class may be thought as a rather "academic" class, whose archetypal examples are the beds of glass beads or sand [7]. The standpoint which is adopted here is that drying must be at least understood for this class of "simple" materials before considering more involved cases. The main transport mechanisms controlling drying in capillary materials are known since the works of Ceaglske and Hougen [7] and Krisher [8]. Capillarity is known to play a key role. Others forces affecting liquid transport are gravity and viscous forces while diffusion is the main mechanism in the gas phase sufficiently below the boiling temperature of water (in this paper, we will restrict ourselves to situations for which temperatures are sufficiently lower than the boiling temperature for total pressure gradients in the gas phase to be negligible).

Another fundamental aspect of drying is the intimate role that the transport of energy may play. Although this is a very important aspect in many drying processes (it is well known that drying is one of the most energy-consuming processes in industry), it may be disregarded in a first step when a fundamental understanding of drying is sought. This implies to consider situations where drying rates are sufficiently low for not imparting significant temperature gradients within the materials. This type of drying is termed "slow drying". Most of this paper is concerned with slow drying, but heat

* Tel.: +33-5-61-28-58-77; fax: +33-5-61-28-58-78.
E-mail address: prat@imft.fr (M. Prat).

1385-8947/02/$ – see front matter
PII: S1385-8947(01)00283-2

transfer aspects will be briefly considered. If one restricts oneself to the simplest situation, a single component liquid must be assumed. However, insights on the evaporation of a binary liquid will be given.

As far as modelling is concerned, first models including capillary effects and vapour transport were developed in the 1950s [9,10]. Although many papers have been published afterwards (see for instance [11]), no significant change in terms of model formulation has been introduced. These models were developed according to phenomenological approaches that consider the porous medium as a fictitious continuum. The effects of the underlying physical phenomena are lumped into effective transport coefficients that must be determined through specific experiments, see Crausse et al. [12] among others. This continuum approach has been placed on a firmer basis through the works of Whitaker [2,13], who essentially derived the same equations as Philip and de Vries or Luikov by a volume averaging technique. However, this later approach rests upon assumptions regarding the phase distribution within the averaging volume that are in fact not verified in certain situations of drying. One interesting feature of the volume averaging technique as developed by Whitaker [13], is, however, the possibility of determining the effective parameters through the solution of closure problems defined over regions representative of the pore microstructure. In this way, a fundamental aspect of the problem which is the disordered nature of the porous microstructure could be analysed. Finally, the motivations for developing models that permit to analyse the influence of the porous microstructure are (at least) twofold. One is the computation of the effective parameters at the scale of a representative volume of the microstructure. A second one is to analyse drying at the scale of the product without assuming a priori the existence of the representative elementary volume that is associated with the continuum approach. Pore network models have been used in both cases. One of their essential aspects is that they can take into account important features of the microstructure. In fact, the use of pore network models for describing drying of porous media is relatively recent. To the best of our knowledge, the first works in which a pore network model is used in the context of drying modelling are those of Daian and Saliba [14] and Nowicki et al. [15]. The motivation was essentially a better understanding of the behaviour of the effective transport parameters as a function of liquid saturation. At the product scale, the studies of the patterns that form during drying and their influence on the drying rates through pore network models are still more recent and began with the drying model proposed by Prat [16]. Since then, two groups have been active in this field, Yortsos and co-workers, see [17], and our group at IMFT, see [18] and references therein. In the present paper, we review the main results obtained so far. In the next section, we begin with the works at the representative elementary volume (REV) scale. The results pertinent at the product scale are discussed in the section that follows. Heat transfer aspects and evaporation of binary liquid are discussed afterwards. Finally, works in progress and some open problems are discussed.

2. Representation of pore space as a pore network

Pore network models are based on a network representation of the porous structure. A sketch of the microstructure of an unconsolidated porous medium is shown in Fig. 1. One can distinguish the pores and the throats. The pores are the voids of relatively large section. The throats are the segments having a minimum cross-section between two pores. As depicted in Fig. 1, an irregular network is obtained by connecting each pore to its neighbour pores. In this network, each pore is also characterised by its coordination, i.e. the number of neighbour pores to which it is connected. Studies are seldom conducted directly on this network. One option is to consider the regular network having the same mean coordination as the irregular one. In fact, some essential properties, such as the exponents governing certain scaling laws [19] are independent of the coordination (in physicist language, the various networks obtained for various mean coordination are said to belong to the same universality class). This explains why most of the studies based on numerical simulations of drying on pore networks were performed on the simplest regular networks (a square network in two-dimensions and a simple cubic lattice in three-dimensions). An other essential ingredient of the network approach is that the width of the throats is not uniform. These widths are distributed according to a given distribution law. This feature is important in relation to capillary and viscous effects. As percolation theory is often the suitable framework for analysing two-phase immiscible displacements governed by capillary effects on networks, networks are often described in terms of percolation

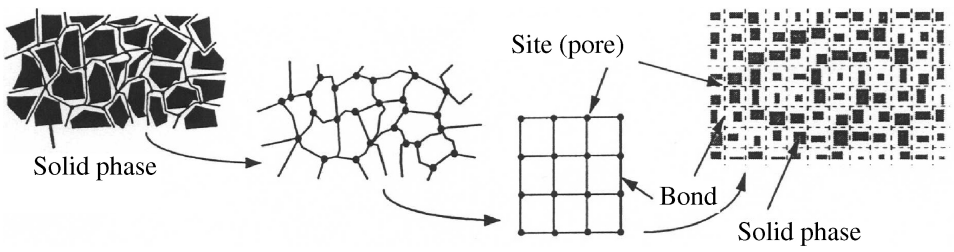

Fig. 1. Modelling of pore space by a network of pores (sites) and throats (bonds).

networks [19]. The pores (the nodes of network) correspond to the "sites" of percolation networks and the throat to the "bonds". In this respect, the aforementioned throat (bond) widths are generally distributed purely randomly. The influence of bond width correlations has not yet been explored in the context of drying. To conclude this section it is important to note that the values of the exponents of the percolation theory are different in two-dimensions and in three-dimensions. This difference reflects differences in connectivity of the pore space. As a result, certain phenomena can only captured by simulations on three-dimensional networks.

3. Pores network models at the REV scale

In this section, the existence of a REV is assumed. Accordingly the continuum approach is assumed to be valid. The pore space within the REV is mapped onto a regular network. Pore network models are then used to compute the effective parameters. Examples of such an approach are presented in [14,15]. Both studies were restricted to isothermal conditions. Cubic pore networks were considered by Daian and Saliba. The distributions of pore volumes and throats widths were obtained from data deduced from sorption and mercury intrusion experiments. Two-dimensional square networks were considered by Nowicki et al. The throat sizes were drawn from a uniform distribution. While Daian and Saliba determined the isothermal mass diffusivity coefficient as a function of saturation, Nowicki et al. determined the relative permeability to liquid, the capillary pressure and effective diffusivity of vapour as functions of liquid saturation and drying history. Daian and Saliba found a reasonable agreement between the predicted and measured diffusivities. The results of Nowicki et al. were essentially illustrative and no comparison with measured macroscopic parameters were presented. The general features of the modelling are, however, essentially identical in both works. In what follows, the work of Nowicki et al., is discussed in more detail. As in most continuum models of drying, a liquid phase continuity equation of the following form was assumed:

$$\varepsilon \frac{\partial S}{\partial t} + \nabla \cdot \boldsymbol{q}_\mathrm{l} = -\frac{\dot{m}}{\rho_\mathrm{l}} \tag{1}$$

where ϵ is the porosity, S the liquid saturation, $\boldsymbol{q}_\mathrm{l}$ the superficial volumetric flux of liquid, $\dot{m}$ the mass rate of drying per unit volume and ρ_l the liquid density. $\boldsymbol{q}_\mathrm{l}$ is related to the pressure gradient in the liquid by (generalised Darcy's law),

$$\boldsymbol{q}_\mathrm{l} = -\frac{k k_\mathrm{rl}}{\mu} \nabla p_\mathrm{l} \tag{2}$$

where k is the permeability of the porous medium, k_rl the relative permeability, which is a function of S and μ the liquid viscosity. Note that gravity effects are neglected here. Because of surface tension acting in curved menisci, the pressure p_g in the gas phase is greater than the pressure in the liquid,

$$p_\mathrm{g} - p_\mathrm{l} = p_\mathrm{c} \tag{3}$$

where p_c is the capillary pressure. Note that the liquid is wetting. In slow drying, p_g is approximately uniform. Therefore,

$$\nabla p_\mathrm{g} \approx 0, \qquad \nabla p_\mathrm{l} \approx -\nabla p_\mathrm{c} \tag{4}$$

The transport of vapour in the gas phase is assumed to be due to diffusion only. The continuity equation of the vapour, assumed to behave as an ideal gas, can be expressed as (under isothermal conditions)

$$\varepsilon \frac{\partial p_\mathrm{v}}{\partial t} = \nabla \cdot (D_\mathrm{eff} \nabla p_\mathrm{v}) + \dot{m} \tag{5}$$

where p_v is the vapour partial pressure and D_eff the vapour effective diffusivity.

The objective of pore network models at the REV scale is essentially to compute parameters such as k, k_rl, p_c, D_eff as a function of S (in the limit of slow rates of drying). Interestingly, however, Nowicki et al. showed that these parameters also depend on the drying rate. This is not surprising since variations of drying rates affect the phase distributions through the competition between capillary and viscous forces (see next section). However, imposing fast drying rates may be thought as inconsistent with the isothermal condition assumed by Nowicki et al. In any case, two main aspects can be distinguished: (i) the computation of the above parameters for a given phase distribution and (ii) the computation of the liquid and gas phase distribution within the network (i.e. the positions of meniscii within the network). Only the main concepts are presented in what follows. The unknowns are the location and the radius of curvature of menisci, the liquid pressure at each meniscus and in each liquid-filled pores, the partial pressure of vapour in each gas-filled pores. These unknowns are determined by solving the equations obtained by expressing the mass balance in each pore and at each meniscus. The volumetric flow rate q_k between adjacent liquid filled pores i and j is expressed as a function of the pressure difference $p_i - p_j$ between pores i and j by

$$q_k = \frac{g_k}{\mu}(p_i - p_j) \tag{6}$$

where g_k is the conductance of the bond connecting pores i and j. The expression of the conductance depends on the shape of the bond and is deduced from the study of Stokes flow through the bond. For instance, if the bond is tube-like,

$$g_k = \frac{\pi r_k^4}{8 L_k} \tag{7}$$

where L_k is the length of the bond and r_k the throat radius.

The mass balance in each liquid filled pore is expressed by Kirchoff's current law,

$$\sum_k q_k = 0 \tag{8}$$

where the sum is over the flow rates through the k bonds that connect to the pore.

In the gas phase, the elementary transport of vapour by diffusion through a bond connecting two gas-filled pores i and j is expressed by, see for instance [20],

$$u_m = \pi r_m^2 \frac{p_a M}{\mathrm{RTL}_m} D \ln\left[\frac{p_a - p_{vi}}{p_a - p_{vj}}\right] \tag{9}$$

where M is the molecular weight of vapour, R the universal gas constant and T the isothermal drying temperature. D is the molecular diffusion coefficient of vapour through air, p_a the ambient gas pressure, p_{vi} (respectively, p_{vj}) the partial pressure of vapour in pore i (respectively, j).

The mass balance in each gas-filled pore is expressed by

$$\frac{\mathrm{d}m_i}{\mathrm{d}t} = \sum_k w_k + \sum_m u_m \tag{10}$$

where m_i is the vapour mass in pore i, w_k the evaporation rate over an evaporating meniscus in adjoining bond k. It is expressed as

$$w_k = \pi r_k^2 \frac{p_a M}{\mathrm{RTL}_k} D \ln\left[\frac{p_a - p_{vi}}{p_a - p_{vek}}\right] \tag{11}$$

where L_k is the distance between the meniscus and pore i, p_{vek} the equilibrium vapour partial pressure at the meniscus, which is related to the meniscus radius of curvature R_k by the Kelvin equation,

$$p_{vek} = p_{vs} \exp\left(-\frac{2\gamma M}{\rho_l R\, \mathrm{TR}_k}\right) \tag{12}$$

where γ is the surface tension.

The mass balance in each bond containing a meniscus is expressed by

$$\frac{\mathrm{d}m_k}{\mathrm{d}t} = \rho_l q_k - w_k \tag{13}$$

while the pressure jump at the meniscus is classically expressed by the Yound–Laplace equation,

$$p_a - p_{lk} = \frac{2\gamma}{R_k} \tag{14}$$

where the liquid is assumed perfectly wetting.These equations are completed by the ideal gas law and an equation relating the radius of curvature to the volume of liquid in a bond where a meniscus is located. This equation depends on the shape of the bond. Biconical bonds were assumed in [15].

The above set of equations was solved numerically by Nowicki et al. for the following initial and boundary conditions. The pore network was completely filled with liquid initially. Periodic boundary conditions were imposed on the sides. The bottom was open to ambient pressure and no evaporation was assumed. Drying took place from top surface. The evaporation flux at top surface was expressed by

$$w_k = k_m(p_{vek} - p_{v\infty}) \tag{15}$$

where k_m is a mass transfer coefficient and $p_{v\infty}$ the vapour partial pressure in the surrounding gas.

The macroscopic parameters are obtained as follows over the network or a sub-region of network (sampling volume in Nowicki et al. terminology). The total liquid and vapour flux through the top surface of the considered region was calculated. The arithmetic mean of the capillary pressure (and the vapour partial pressure) along the top and bottom surfaces of the region were determined. The relative permeability and the effective diffusivity were calculated from the following finite difference approximations

$$k_{rl} = -\mu \frac{q_l}{k} \frac{L}{\Delta p_c}, \qquad D_{eff} = -\mu \frac{RT\rho_g q_g}{M} \frac{L}{\Delta p_v} \tag{16}$$

where L is the length of the considered region, Δp_c the capillary pressure difference across the region (difference between the top and bottom capillary pressure arithmetic means) and Δp_v the vapour partial pressure difference across the region.

As the saturation S in the network and/or the sub-region can be evaluated at each invasion step, the evolution of k_{rl}, D_{eff}, and the mean capillary pressure can be plotted as a function of S. Examples of such plots are presented by Nowicki et al. The computations were performed over 30×30 networks, which is a relatively small size. It would be interesting to repeat this type of calculation over three-dimensional networks of larger size.

4. Pore network models at the product scale

As mentioned in the introduction, the objectives of a pore network at the product scale are twofold. One is to predict the phase distribution during drying. A second is to study the evolution of the drying rates. Naturally, the two objectives are not independent since the drying rates are intimately associated with the evolution of the phase distribution within the sample. To the best of our knowledge, the first pore network model of drying at the product scale is the one proposed by Prat [16]. This model, which will be recalled below, combines invasion percolation concepts and computation of the diffusive transport of vapour in the gas phase according to a discrete approach similar to that discussed in the previous section (Eqs. (9) and (10)).

4.1. Invasion percolation

Invasion percolation is a dynamic percolation process introduced to model the slow immiscible displacement of a wetting fluid by a non-wetting one in a porous medium [21,22]. Drying and drainage present obvious analogies

Both of them are characterised by the movement of meniscii through the porous medium and progressive invasion of the medium by the non-wetting fluid (the gas in drying). Naturally, drying is also different from drainage owing to the additional effect of mass transfer in the gas phase, which actually drives the process. These differences are discussed below. The analogy with drainage was first evidenced by Shaw [23] in an experiment performed with a quasi two-dimensional packing of very small particles. He observed invasion fronts that strongly resembled drainage invasion percolation front (due to the uncertainty in the data, the formal analogy with a drainage front could not be demonstrated). From the work of Lenormand et al. [24], it is known that drainage patterns are controlled (when gravity forces are ignored) by two-dimensionless numbers, the viscosity ratio of the two fluids and the capillary number Ca which is the ratio of viscous forces to capillary ones (the lower the capillary number, the greater the capillary forces). In (slow) drying, capillary forces are always important. For this reason, it is of interest to consider first the "asymptotic" case where capillarity effects dominate. This case corresponds to invasion percolation patterns in the phase diagram proposed by Lenormand et al. [24]. The invasion percolation algorithm is recalled in what follows. Consider a regular network of pores and bonds. The network is initially completely filled with liquid. The width of the bonds is randomly distributed according to a given distribution law. For simplicity, assume tube-like bond of radius r_b. Assuming a perfectly wetting fluid, the threshold capillary pressure of a bond is given by (Young–Laplace equation)

$$p_{cb} = \frac{2\gamma}{r_b} \tag{17}$$

The non-wetting fluid can enter the network through the top surface of network (entrance surface). The wetting fluid can escape the network through the bottom surface of network (exit surface). The fluids cannot escape or enter through the sides. The stable position of a meniscus is at the entrance of a bond. The algorithm describing invasion percolation can be stated as follows:

1. Among all the bonds at the entrance of which a meniscus is located, select the one which has the lowest threshold capillary pressure.
2. Invade the bond selected in step 1 together with its adjacent pore.
3. End the invasion process when the invading fluid reaches a pore on the exit surface.

This algorithm describes invasion percolation without trapping. In fact, when this algorithm is used, regions of wetting fluid become completely surrounded by the invading non-wetting fluid. Because of the incompressibility of the wetting fluid, these regions, called "disconnected clusters", cannot be invaded. Hence, the algorithm pertinent to drainage should incorporate the trapping rule: the disconnected clusters cannot be invaded, i.e. the interfacial bonds of disconnected clusters (the bonds of disconnected clusters at the entrance of which meniscii are located) are removed from the list of interfacial bonds in step 1. Fig. 2a shows a typical phase distribution obtained with the invasion percolation algorithm with trapping on a regular square network. Note the disconnected clusters of various size (the maximum size is imposed by the size of network). There are considerable evidences that invasion percolation with trapping adequately describes slow drainage in a porous medium, see for instance [25].

4.2. Phase distributions, drying algorithm, influence of gravity and viscosity effects

The phase distribution of Fig. 2a is to be compared with the phase distribution (shown in Fig. 2b) obtained with the drying algorithm proposed by Prat [16]. As can be seen from Fig. 2a, the striking difference between drying and drainage is that the disconnected clusters can be invaded in drying. The drying algorithm used for obtaining the phase distribution depicted in Fig. 2b, can be described as follows:

1. every cluster present in the network is identified,
2. the bond connected to the already invaded region which has the lowest threshold capillary pressure is identified for each cluster,
3. the evaporation flux at the boundary of each cluster is computed,
4. for each cluster, the mass loss corresponding to the evaporation flux determined in step 3 is assigned to the bond identified in step 2,
5. the bond (as well as the adjacent pore) eventually invaded is that which is the first to be completely drained among the bonds selected in step 2,
6. the phase distribution within the network is updated.

In this model, the liquid is a single component liquid. The gas phase is a binary mixture consisting of the vapour of the liquid and an inert component. Kelvin effect is neglected. The evaporation flux (step 3) are determined from the computation of the molar fractions in the vapour phase. The computational method is similar to that presented in the previous section, Eqs. (9)–(11), with the additional simplifying assumption of a quasi-steady diffusive transport. In this simulation, vapour was allowed to escape through the top edge of network. Zero flux conditions were imposed on the three remaining edges. As reported in [26], comparisons with experiments on etched networks showed that this model captured the essential features of the phase distribution evolution in slow drying.

As reported in [27], this model has also been used to perform simulations of drying on a three-dimensional network. A simple cubic network was considered. Vapour could escape through one of the surface of network. Numerical visualisations of the liquid–gas interface within the network during drying led to distinguish three main stages. In the first stage the gas preferentially invades the region of the open

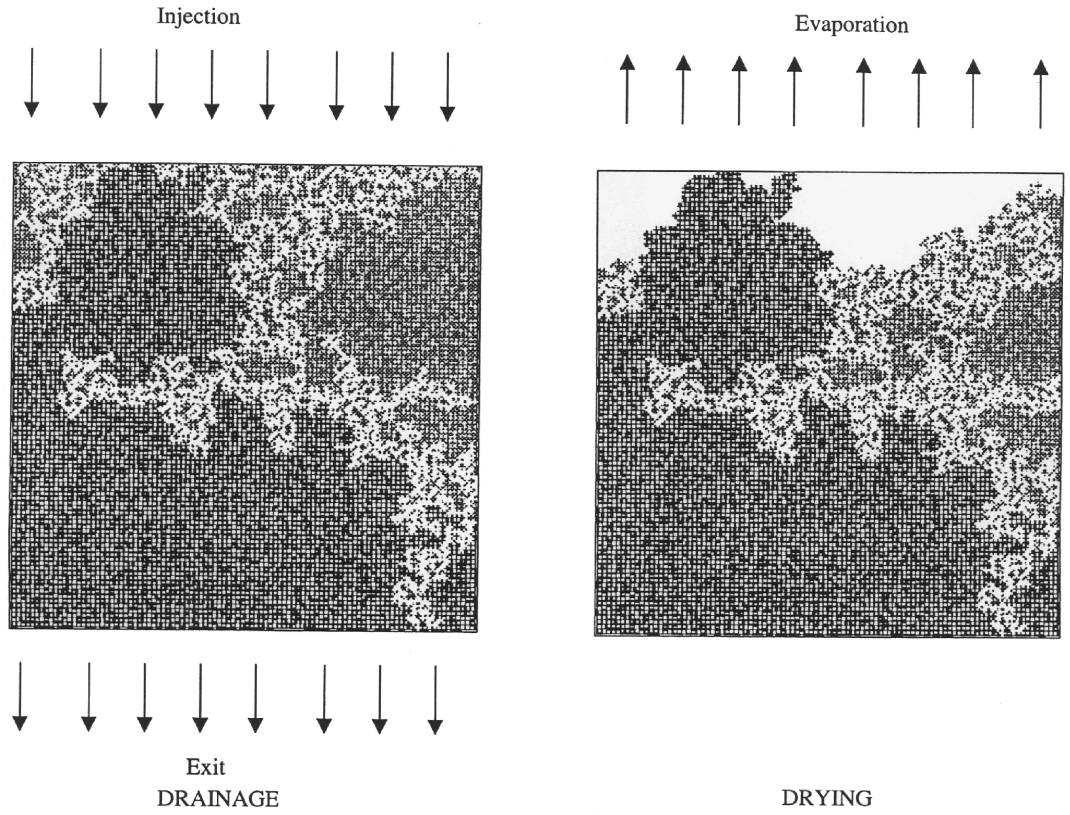

Fig. 2. (a) Phase distribution predicted with the invasion percolation algorithm with trapping in a 100 × 100 network. The liquid phase is in black. The gas phase is in white. Note the numerous disconnected clusters. (b) Phase distribution predicted with the slow drying pore network model in the same 100 × 100 network as for (a). The liquid phase is in black. The gas phase is in white. Note the occurrence of a dry zone along the open (top) surface (adapted from [37]).

face. Irregular fractal patterns typical of invasion percolation were obtained as shown in Fig. 3a. The second stage is characterised by an invasion of the sample which seems statistically homogeneous and isotropic. A typical visualisation for this stage is shown in Fig. 3b. The third stage is characterised by the full drying of the sample through an evaporation process sweeping the network from the open to the opposite surface. A typical visualisation for this stage is shown in Fig. 3c. Disconnected clusters are clearly visible in Fig. 3c. This suggests that the liquid phase is in fact distributed in the form of disconnected clusters when the third stage starts. Hence, in terms of phase distribution evolution, drying can be defined as a progressive fragmentation and erosion process of the liquid phase. Initially, the liquid phase forms a single cluster spanning the network. When the third phase starts, there is no network spanning liquid cluster anymore but a large numbers of isolated liquid clusters of various size.

The pore network drying model described above takes into account capillarity only as a force acting on the liquid. It is well known that viscous forces and gravity forces may also be important. Incorporating gravity effects in the model is an easy matter. Taking into account viscous effects is more involved. In both cases, the idea is to take into account the variation of the liquid pressure induced either by gravity effects or by viscosity effects. The method, which was first proposed by Wilkinson [28], amounts to considering the following bond invasion potential,

$$Q_b(\boldsymbol{x}) = \frac{2\gamma}{r_b} - (P_g - P_l(\boldsymbol{x})) \tag{18}$$

where r_b is the radius of the bond (throughout this paper a perfectly wetting liquid is assumed), $\boldsymbol{x}$ is a position vector, P_g the total pressure in the gas phase, which is assumed to be constant and P_l is the pressure in the liquid phase. The drying algorithm is identical to the one listed above except that step 2 now reads: the bond connected to the already invaded region which has the lowest invasion potential is identified for each cluster.

The additional problem is to determine P_l at each step of invasion. When gravity effects are important and viscous effects can be disregarded, the liquid pressure (P_l) distribution is hydrostatic and therefore known analytically. When viscous effects are to be taken into account, the pressure in the liquid phase must be determined numerically. The method [29] is similar to that presented in the previous section, Eqs. (6)–(8).

The influence of gravity has been studied by Laurindo and Prat [26] and Prat and Bouleux [18]. Two main situations can be distinguished. When the open surface of network is the top surface, gravity acts as a stabilising force. This leads

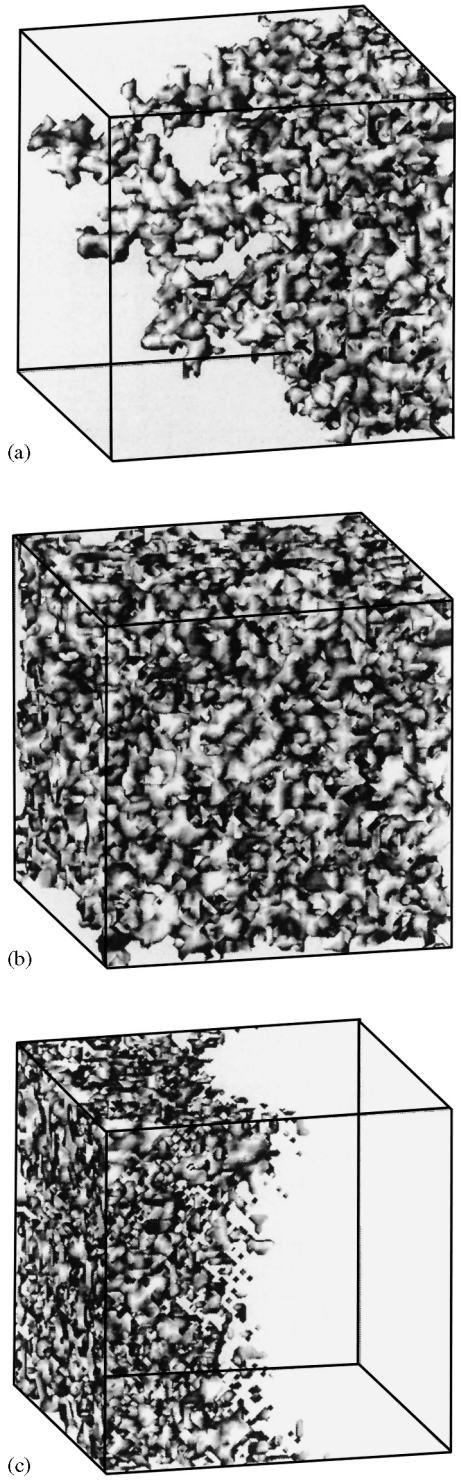

Fig. 3. Liquid–gas interface within a cubic network at three stages of drying. The open surface is the (hidden) right-hand surface in the figure (adapted from [27]). Viscous and gravity effects are negligible in this simulation.

to the formation of drying front as shown in Fig. 4a. When the open surface is the bottom surface, gravity acts as a destabilising force. This leads to the formation of a single branch in a first step of drying as depicted in Fig. 4b.

As first noted by Shaw [23], viscous effects are stabilising. Thus, drying fronts resembling gravity stabilised fronts are expected. Drying fronts stabilised by viscosity were studied by Shaw [23], Tsimpanogiannis et al. [17] and Prat and Bouleux [18].

4.3. Phase diagram

The pattern to be observed in a given experiment can be predicted by comparing the length L of the sample with the characteristic width L_{cap} of the "viscous" front and the characteristic width L_g of the "gravity" front. Estimates of L_g and L_{cap} as functions of the various parameters controlling drying are derived in [26] or [18] using macroscopic concepts,

$$\frac{L_g}{\bar{r}} \approx B^{-1} \tag{19}$$

where B is the Bond number defined here as $B^{-1} = 2\gamma \cos\theta/\bar{r}^2 \rho_L g$ (the Bond number describes the relative importance of gravity over capillary forces). γ is the surface tension, θ the wetting angle and $\bar{r}$ is an average pore size. ρ_L is the liquid density and g the acceleration of gravity.

$$\frac{L_{cap}}{\bar{r}} \approx \frac{k}{\bar{r}^2} \mathrm{Ca}^{-1} \tag{20}$$

where k is the porous medium permeability. Ca is the capillary number, which characterises the competition between the viscous and the capillary forces. Ca is defined by $\mathrm{Ca}^{-1} = 2\gamma \cos\theta/\mu_L v$, where v is a characteristic liquid filtration velocity and μ_L the liquid dynamic viscosity. v is identified with the filtration velocity at the onset of the process. Under these circumstances, one may define v as

$$v = \frac{e}{\rho_L} \tag{21}$$

where e is the evaporation flux density at the open surface of medium.

When L_{cap} and L_g are greater than L, the system is too small for "feeling" the influence of gravity or viscosity. The process is dominated by capillarity and a capillary fingering pattern (Fig. 2b or Fig. 3) is expected. When L_{cap} or L_g is smaller than L, a front is expected (in this section, gravity destabilising cases are not considered). As under standard constant external drying conditions e decreases during the process, L_{cap} progressively increases. Therefore, in some cases, one may have $L_{cap} < L$ and therefore a viscous front at the beginning of the process whereas later L_{cap} may become larger than L, which corresponds to a capillarity dominated regime. The various patterns that can be expected are summarised in Fig. 5.

4.4. Dry patch phenomenon

It is also interesting to observe that the phenomenon of dry and wet patches is captured by the pore network

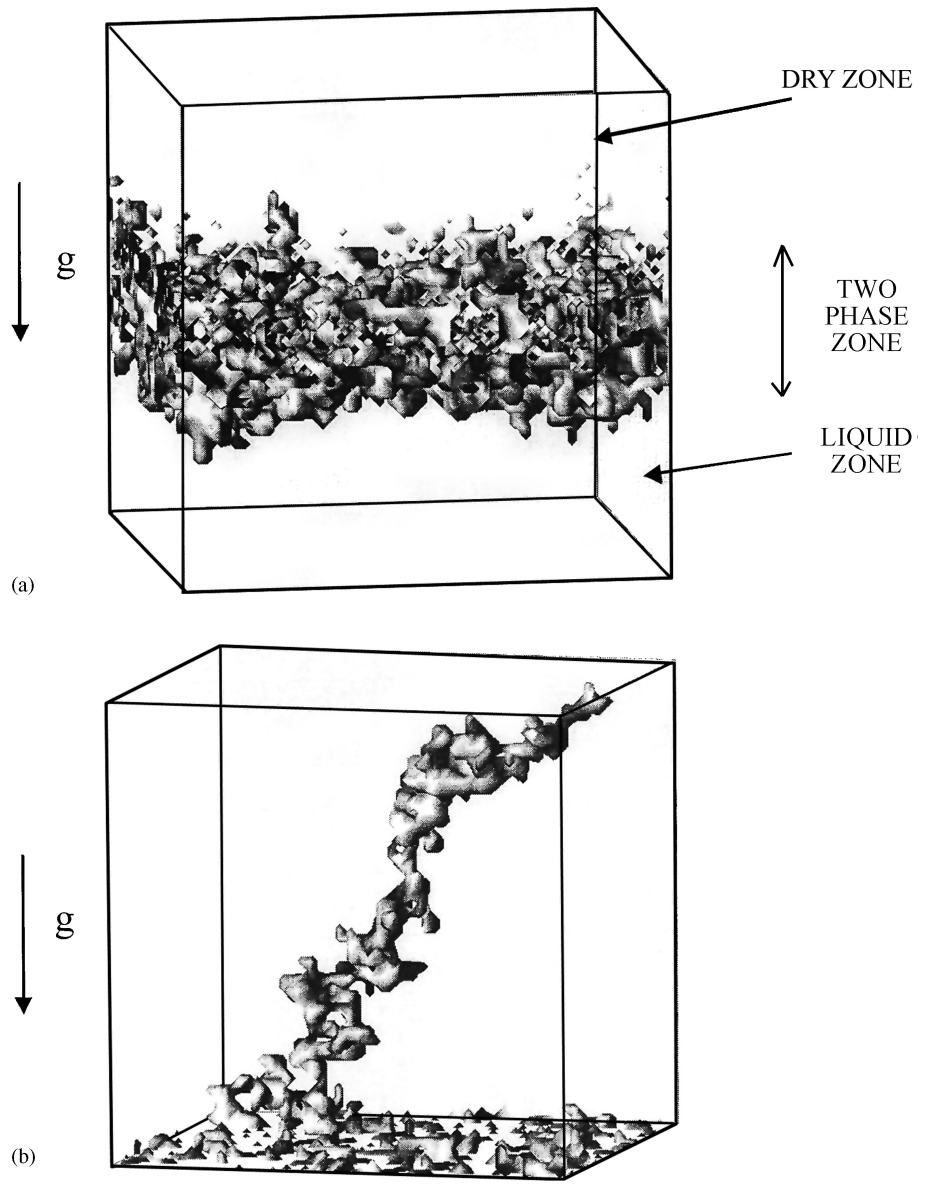

Fig. 4. (a) Liquid–gas interface in a cubic network when gravity acts as a stabilising force. There are three main zones. A dry zone near the open (top) surface. A liquid zone occupying the lower part of network. A (two-phase) front region in between where both gas and liquid phases are macroscopically continuous (in 3D). (b) Liquid–gas interface in a cubic network when gravity acts as a destabilising force. There are three main steps as described in [26]. This figure corresponds to the first step which is characterised by a single branch growing upward. The open surface where evaporation takes place is the bottom surface.

model as shown in Fig. 6. In the context of the present model, dry patches are a consequence of an invasion process dominated by capillarity. It is perhaps worth mentioning that, in our model, the porous structure is macroscopically homogeneous. Naturally, large scale structural heterogeneities (pore size correlation, variation of local porosity), that may be present in a real system, should certainly contribute to the formation of dry patches. However, our result clearly show that large scale structural heterogeneities are not necessary to observe dry patches.

4.5. Drying rates

From a practical standpoint, prediction of drying rates is certainly the most important objective of a drying model. Comparisons between experiments on two-dimensional etched networks and simulations based on the pore network model described above were reported in [30]. The agreement was only qualitative. The drying rates predicted by the simulations were systematically lower than measured. This is due to roughness and corner film flows, a transport mechanism in liquid phase which is not incorporated in

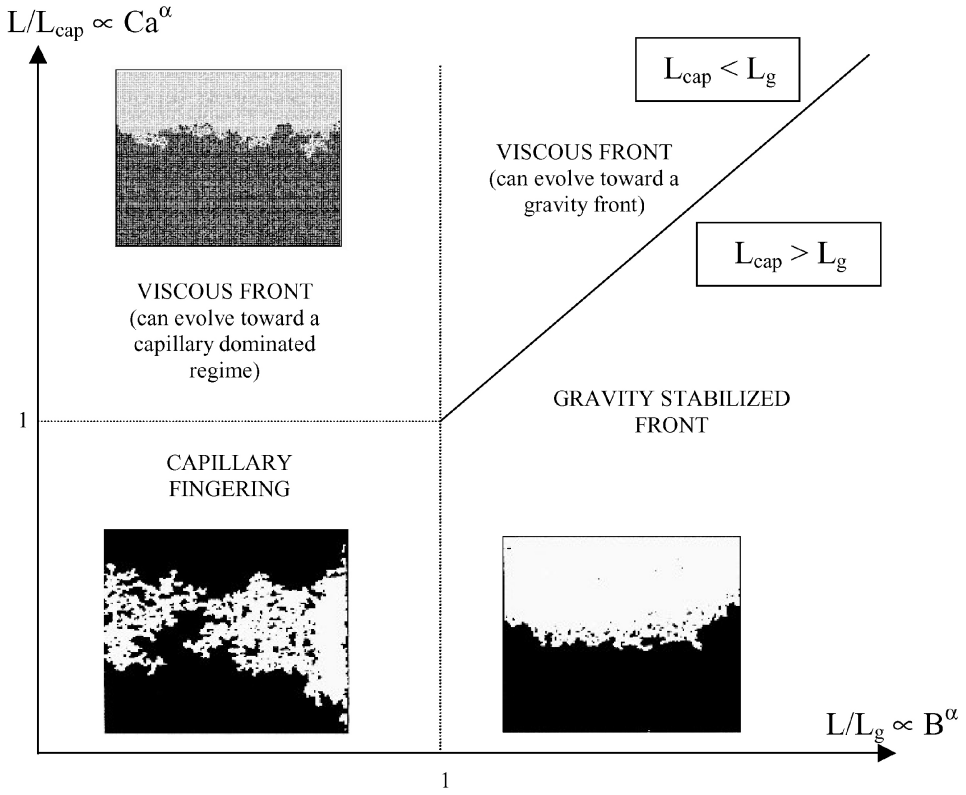

Fig. 5. Drying phase diagram (gravity destabilising regimes are not considered).

the simulations. A schematic of film flows in a bond of rectangular cross-section is shown in Fig. 7.

Although film flows need to be incorporated in the model for quantitative predictions, it is interesting to note that the present version of the model is qualitatively consistent with the classic description of convective drying in three periods first proposed by Krisher [8]. In particular, the model captures the constant rate period (CRP), which is perhaps the most puzzling feature of drying of capillary porous media. Fig. 8 shows the drying curve obtained by simulation

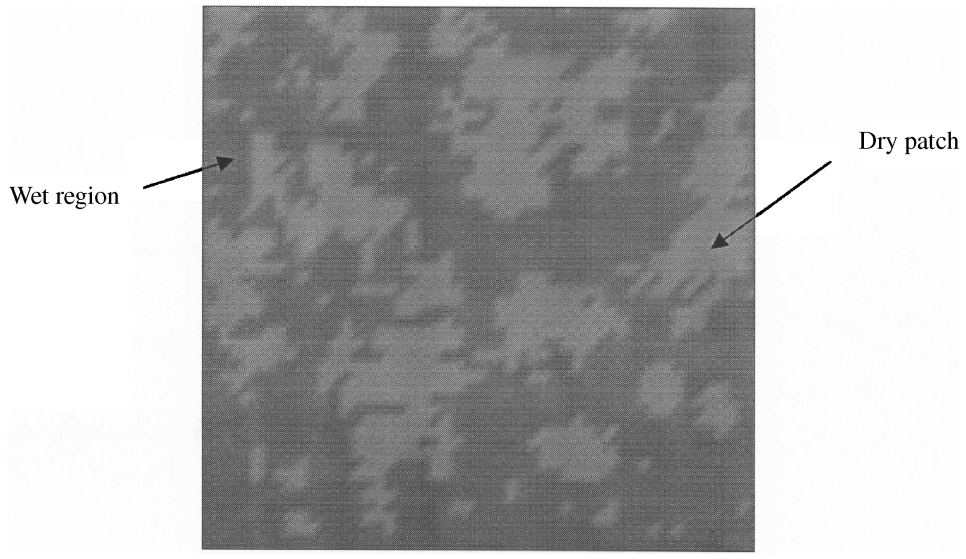

Fig. 6. Occurrence of dry and wet patches at the open surface of network. Liquid in dark gray, gas in light gray. This result has been obtained by simulation over a $51 \times 51 \times 51$ network (adapted from [27]).

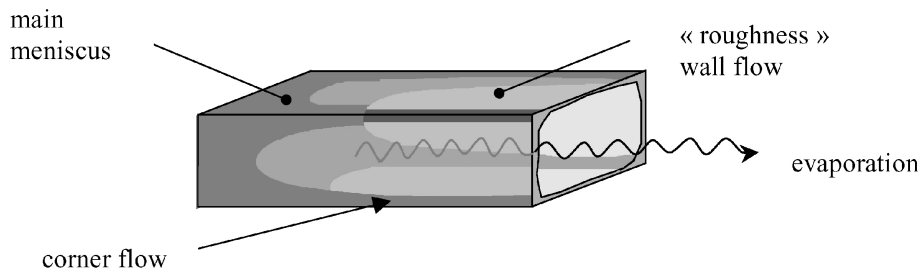

Fig. 7. Schematic of liquid film flows in corners and along the pore walls in a duct whose bulk has been invaded by the gas phase. These flows are due to secondary capillary effects.

over a 51 × 51 × 51 network as reported in [27]. Gravity and viscous effects were negligible in this simulation. It is perhaps worth pointing out that the CRP can be captured with three-dimensional network only. The drying-curve for two-dimensional network does not show a significant CRP. This is due to trapping which is much more effective in two-dimensions (in others terms, the fact that, in three dimensions, the liquid phase remains connected over distance of the order of the sample size during a significant part of drying is an essential feature here). More detail can be found in [27].

4.6. Evaporation of a binary liquid

A pore network model of evaporation of a binary liquid mixture into a ternary gas phase was developed by Freitas and Prat [31]. The system considered was a two-dimensional network initially saturated with a 2-propanol water mixture that evaporated into air at a moderate temperature. The model was applied to study the influence of surface tension gradients induced by composition variations of the liquid on the phase distribution within a capillary porous medium. The numerical simulations showed that the surface tension gradients led to the accumulation of liquid near the open edge of the network. This surface tension gradient effect was only significant for weakly disordered porous media. In this case, the results indicate that patterns of the destabilising gravity type can be expected. These results are consistent with experimental results available in the literature as discussed in de Freitas and Prat [31].

4.7. Influence of heat transfer

A pore network model of drying including heat transfer modelling has been developed by Plourde and Prat [32]. The modelling of heat transfer is performed over a finer network than the pore network in order to model heat transfer in the solid phase. The results indicate effects of surface tension variation induced by temperature variations that are analogous to those induced by the composition variations mentioned in the previous paragraph. Depending on the orientation of temperature gradients, destabilised invasion or stabilised invasion patterns are obtained when the disorder of porous medium is sufficiently low. Others examples of pore network models including liquid–vapor phase change and heat transfer can be found in [33,34].

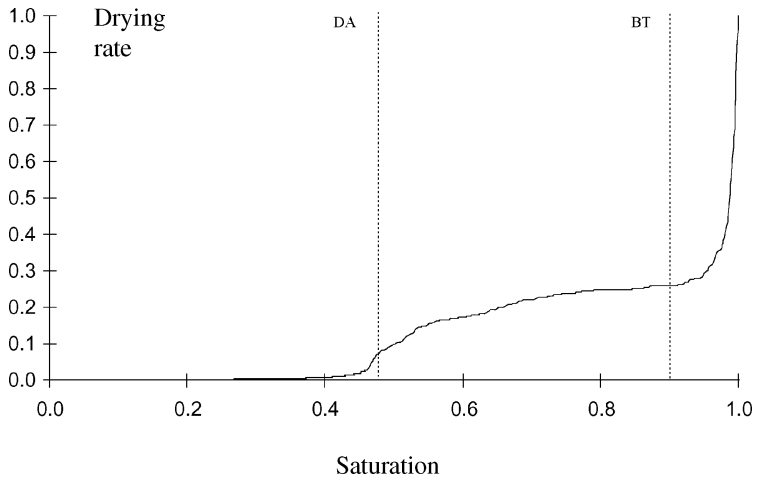

Fig. 8. Drying curve obtained by numerical simulation over a 51 × 51 × 51 pore network. Constant external convective drying conditions are imposed. Gravity and viscous effects are negligible compared to capillary effects. The drying rate is normalised by the drying rate at $t = 0$ (adapted from [27]).

5. Open problems

Although important developments have been made in the field of pore network modelling of drying for about 10 years, there is still a lot to do. Film flows must be taken into account at the REV scale as well as at the product scale. In principle, this does not pose any particular problem, at least under isothermal conditions. Here again, one can rely on what has been done in the related domain of immiscible displacements in porous media, see for instance [35]. In the spirit of the work of Nowicki et al. [15], it would be interesting to study the behaviour of the effective parameters from simulations on three-dimensional networks. As mentioned before, a first pore network model of drying including heat transfer has been developed [32]. This model does not take into account film flows. Modelling of film flows in the presence of heat transfer is to be done.

At the product scale, the models described in the present paper are based on the rule that only one bond is invaded at each step of invasion. This is consistent with the assumption of "slow" drying. For faster drying rates, displacements can occur in more than one pore, as observed in the experiments of Tsimpanogiannis et al. [17]. Although the influence of this effect on the average behaviours is still unclear, it would be better to incorporate this effect in the model. The Kelvin effect, Eq. (12), was taken into account by Nowicki et al. but not in the models at the product scale. It would be interesting to assess the influence of this effect through pore network simulations. An important issue concerns the relatively simple structure of the pore networks used in all the simulations discussed in the present paper. This structure is suitable for capillary porous materials showing a narrow pore (bond) size distribution. Network models for materials having a broad pore-size distributions have been proposed in the literature, see for instance [36]. It would be interesting to model drying over this type of network.

In this review, we mainly concentrated on pore network models. We have indicated that the suitable framework for analysing the results was percolation theory and its variants (invasion percolation, invasion percolation in a gradient). There are also fundamental issues associated with these theories that would deserve to be explored by statistical studies based on pore network simulations (in the spirit of the works of Tsimpanogiannis et al. [17] and Prat and Bouleux [18]).

6. Conclusions

The results recalled in this paper show that the recent developments in network modelling of drying have led to significant advances. Coupled with percolation theories they offer a consistent framework for studying drying. They represent one interesting alternative for studying problems that cannot be handled by continuum approaches. They also offer a possibility for predicting the effective parameters of continuum models when these models can be considered as valid. In our opinion, new advances of both a scientific and practical nature can be expected to occur in the next future thanks to network models.

Acknowledgements

This paper could not have been written without the help of the graduate or ex-graduate students of our group, F. Bouleux, D.S. de Freitas, C. Figus, J. Laurindo and Y. Le Bray. This help is gratefully acknowledged. Financial supports from Institut Français du Pétrole is also gratefully acknowledged.

References

[1] G.W. Scherer, Theory of drying, J. Am. Ceram. Soc. 73 (1990) 3–14.
[2] S. Whitaker, Simultaneous Heat, Mass and Momentum Transfer in Porous Media: A Theory of Drying, Advances in Heat Transfer, Vol. 13, Academic Press, New York, 1977, pp. 119–203.
[3] O.A. Plumb, Transport Phenomena in Porous Media: Modeling the Drying Process, Handbook of Porous Media, Marcel Dekker, New York, 2000, pp. 755–785.
[4] R.B. Keey, Drying: Principles and Practice, Pergamon Press, Oxford, 1972.
[5] A.W. Adamson, Physical Chemistry of Surfaces, Wiley/Interscience, New York, 1967.
[6] F.A.L. Dullien, Porous Media, Fluid Transport and Pore Structure, Academic Press, New York, 1992.
[7] N.H. Ceaglske, O.A. Hougen, Drying granular solids, Ind. Eng. Chem. 29 (1937) 805–813.
[8] O. Krisher, Die Wissenshaftlichen Grundlagen Der Trocknungstecknick, Vol. 1, Springer, Berlin, 1963, p. 298.
[9] J.R. Philip, D.A. deVries, Moisture movement in porous materials under temperature gradients, Trans. Am. Geophys. Un. 38 (1957) 222–232.
[10] A.V. Luikov, Experimentelle und Theorestische der Trocknung, VEB, Berlin, 1958.
[11] S. Bories, Recent advances in modelisation of coupled heat and mass transfer in capillary-porous bodies, in: Proceedings of the Sixth International Drying Symposium, 1988, pp. KL.47–KL.61.
[12] P. Crausse, G. Bacon, S. Bones, Etude fondamentale des transferts couplés chaleur-masse en milieu poreux, Int. J. Heat Mass Transf. 24 (6) (1981) 991–1004.
[13] S. Whitaker, Coupled Transport in Multiphase Systems: A Theory of Drying, Advances in Heat Transfer, Vol. 31, Academic Press, New York, 1998, pp. 1–103.
[14] J.F. Daian, J. Saliba, Détermination d'un réseau aléatoire de pores pour modéliser la sorption et la migration d'humidité dans un mortier de ciment, Int. J. Heat Mass Transf. 34 (8) (1991) 2081–2096.
[15] S.C. Nowicki, H.T. Davis, L.E. Scriven, Microscopic determination of transport parameters in drying porous media, Drying Technol. 10 (4) (1992) 925–946.
[16] M. Prat, Percolation model of drying under isothermal conditions in porous media, Int. J. Mult. Flow 19 (1993) 691–704.
[17] I.N. Tsimpanogiannis, Y.C. Yortsos, S. Poulou, N. Kanellopoulos, A.K. Stubos, Scaling theory of drying in porous media, Phys. Rev. E 59 (4) (1999) 4353–4365.
[18] M. Prat, F. Bouleux, Drying of capillary porous media with stabilized front in two-dimensions, Phys. Rev. E 60 (5 PTB) (1999) 5647–5656.

[19] D. Stauffer, A. Aharaony, Introduction to Percolation Theory, Taylor & Francis, London, 1992.
[20] R.B. Bird, W.E. Stewart, E.N. Lightfoot, Transport Phenomena, Wiley, New York, 1960.
[21] R. Lenormand, S. Bones, Description d'un mécanisme de connexion de liaisons destiné à l'étude du drainage avec piégeage en milieu poreux, C. R. Acad. Sci. Ser. B 291 (1980) 279–280.
[22] D. Wilkinson, J.F. Willemsen, Invasion percolation: a new form of percolation theory, J. Phys. A 16 (1983) 3365–3376.
[23] T.M. Shaw, Drying as an immiscible displacement process with fluid counterflow, Phys. Rev. Lett. 59 (15) (1987) 1671–1674.
[24] R. Lenormand, E. Touboul, C. Zarcone, Numerical models and experiments on immiscible displacements in porous media, J. Fluid Mech. 189 (1988) 165–187.
[25] R. Lenormand, C. Zarcone, Invasion percolation in an etched network: measurement of a fractal dimension, Phys. Rev. Lett. 54 (1985) 2226–2229.
[26] J.B. Laurindo, M. Prat, Numerical and experimental network study of evaporation in capillary porous media. Phase distributions, Chem. Eng. Sci. 51 (23) (1996) 5171–5185.
[27] Y. Le Bray, M. Prat, Three dimensional pore network simulation of drying in capillary porous media, Int. J. Heat Mass Transf. 42 (1999) 4207–4224.
[28] D. Wilkinson, Percolation model of immiscible displacement in the presence of buoyancy forces, Phys. Rev. A 30 (1) (1984) 520–531.
[29] F. Bouleux, Approche discrète de l'évaporation en milieu poreux, Etude de fronts stabilisés par les forces de gravité ou de viscosité en deux dimensions, INPT Thesis, 1999.
[30] J.B. Laurindo, M. Prat, Numerical and experimental network study of evaporation in capillary porous media. Drying rates, Chem. Eng. Sci. 53 (12) (1998) 2257–2269.
[31] D.S. de Freitas, M. Prat, Pore network simulation of evaporation of a binary liquid from a capillary porous medium, Transport Porous Med. 40 (2000) 1–25.
[32] F. Plourde, M. Prat, Pore network simulations of drying of capillary porous media, Influence of thermal gradient, Int. J. Heat Mass Transf., submitted for publication.
[33] C. Satik, Y.C. Yortsos, A pore network study of bubble growth in porous media driven by heat transfer, J. Heat Transf. Trans. ASME 118 (1996) 455–462.
[34] C. Figus, Y. Le Bray, S. Bories, M. Prat, Heat and mass transfer with phase change in a porous structure partially heated. Continuum model and pore network simulations, Int. J. Heat Mass Transf. 42 (1999) 2257–2569.
[35] M. Sahimi, Flow and Transport in Porous Media and Fractured Rock, VCH, Weinheim, 1995.
[36] A.V. Neimark, Multiscale percolation systems, Sov. Phys. JETP 69 (4) (1989) 786–791.
[37] M. Prat, Isothermal drying of non-hygroscopic capillary-porous materials as an invasion percolation process, Int. J. Mult. Flow. 21 (1995) 875–892.